Identification of Phosphorylation Sites on AChR δ-Subunit Associated with Dispersal of AChR Clusters on the Surface of Muscle Cells †

ARTICLE *in* BIOCHEMISTRY · NOVEMBER 1998

Impact Factor: 3.02 · DOI: 10.1021/bi9802824 · Source: PubMed

6 AUTHORS, INCLUDING:

Nan-Shan Chang
National Cheng Kung University
132 PUBLICATIONS **2,038** CITATIONS
SEE PROFILE

Marina Gelman
Rigel
13 PUBLICATIONS **479** CITATIONS
SEE PROFILE

Joav Prives
Stony Brook University
38 PUBLICATIONS **1,372** CITATIONS
SEE PROFILE

Identification of Phosphorylation Sites on AChR δ-Subunit Associated with Dispersal of AChR Clusters on the Surface of Muscle Cells†

Anjaruwee S. Nimnual,‡ Weise Chang,‡,§ Nan-Shan Chang,|| Anthony F. Ross,‡,⊥ Marina S. Gelman,‡,# and Joav M. Prives*,‡

Department of Pharmacological Sciences, State University of New York at Stony Brook, Stony Brook, New York 11794, and Laboratory of Molecular Immunology, Guthrie Research Institute, 1 Guthrie Square, Sayre, Pennsylvania 18840

Received February 4, 1998; Revised Manuscript Received August 8, 1998

ABSTRACT: The innervation of embryonic skeletal muscle cells is marked by the redistribution of nicotinic acetylcholine receptors (AChRs) on muscle surface membranes into high-density patches at nerve−muscle contacts. To investigate the role of protein phosphorylation pathways in the regulation of AChR surface distribution, we have identified the sites on AChR δ-subunits that undergo phosphorylation associated with AChR cluster dispersal in cultured myotubes. We found that PKC-catalyzed AChR phosphorylation is targeted to Ser^{378}, Ser^{393}, and Ser^{450}, all located in the major intracellular domain of the AChR δ-subunit. Adjacent to one of these sites is a PKA consensus target site (Ser^{377}) that was efficiently phosphorylated by purified PKA in vitro. The PKC activator 12-*O*-tetradecanoylphorbol-13-acetate (TPA) and the phosphoprotein phosphatase inhibitor okadaic acid (OA) produced increased phosphorylation of AChR δ-subunits on the three serine residues that were phosphorylated by purified PKC in vitro. In contrast, treatment of these cells with the PKA activator forskolin, or with the cell-permeable cAMP analogue 8-bromo-cAMP, did not alter the phosphorylation state of surface AChR, suggesting that PKA does not actively phosphorylate the δ-subunit in intact chick myotubes. The effects of TPA and OA included an increase in the proportion of surface AChR that is extracted in Triton X-100, as well as the spreading of AChR from cluster regions to adjacent areas of the muscle cell surface. These findings suggest that PKC-catalyzed phosphorylation on the identified serine residues of AChR δ-subunits may play a role in the surface distribution of these receptors.

Aggregation of nicotinic acetylcholine receptors (AChRs) at postsynaptic regions of muscle cell membranes is a prominent feature of the formation of neuromuscular junctions, and the maintenance of high AChR densities at these sites is crucial for transmission of impulses across these chemical synapses (*1*). Studies in nerve−muscle co-cultures have demonstrated that induction of AChR clustering upon innervation involves the redistribution of preexistent surface AChR to subneuronal membrane regions (*2*). Moreover, AChR also undergoes spontaneous clustering in the absence of neuronal intervention, and the formation of nerve-induced AChR clusters at the sites of neuronal contact is accompanied by the dispersal of clusters located in extrasynaptic regions (*3*).

The neuronal induction of AChR clustering can be mimicked by the addition to cultured muscle cells of soluble neural factors (for reviews, see *4*, *5*) including embryonic brain extract (BE) (*6*−*8*) or one of its components, agrin, a protein secreted by motor nerve endings (*4*, *9*), and shown to activate a receptor-like tyrosine kinase in muscle cells (*10*, *11*). Agrin-induced AChR aggregation is associated with an increase in tyrosine phosphorylation of subsynaptic intracellular proteins including AChR subunits (*10*−*15*). Conversely, inhibitors of tyrosine phosphorylation block agrin-dependent AChR clustering (*15*, *16*). In addition, TPA and other PKC activators have been shown to increase AChR phosphorylation and to cause AChR declustering in myotubes, suggesting that surface AChR distribution in the plasma membrane may be modulated by PKC-catalyzed phosphorylation (*17*, *18*). Together, these findings suggest that the formation and dispersal of AChR clusters may be regulated by discrete phosphorylation pathways.

AChR clusters overlie cytoskeletal regions of specialized composition (*19*). Clustered AChR has been shown by detergent extraction and lateral mobility measurements to be selectively anchored to cytoskeletal components, while diffusely distributed AChR is unattached and more highly mobile in the plane of the membrane (*20*−*22*). Recent studies indicate that agrin-induced AChR clustering is associated with localized cytoskeletal rearrangements (*11*, *23*−*25*), and agrin treatment of cultured myotubes induces

† This work was supported by grants from the NIH (NS 25945), NSF (IBN9723145), and MDA.

* Corresponding author: Department of Pharmacological Sciences, Health Sciences Center, State University of New York at Stony Brook, Stony Brook, NY 11794. Telephone: (516) 444-3139. Fax: (516) 444-3218.

‡ State University of New York at Stony Brook.

§ Present address: Laboratory of Cellular Biology, National Institute on Deafness and Other Communication Disorders, NIH, Rockville, MD 20850.

|| Guthrie Research Institute.

⊥ Present address: College of Chiropractic, University of Bridgeport, Bridgeport, CT 06601.

Present address: Department of Biological Sciences, Stanford University, Palo Alto, CA 94305-5020.

10.1021/bi9802824 CCC: $15.00
Published on Web 09/26/1998

the increased retention of surface AChR on the detergent-insoluble cytoskeletal framework (*26*). Thus, there is substantial evidence that the spatial redistribution of surface AChR induced by neuronal factors is accompanied by altered interactions of AChR with adjacent structural elements. These interactions may in turn be regulated by phosphorylation of the AChR itself or of associated cytoskeletal proteins.

The present study was aimed at characterization of cellular mechanisms that mediate AChR phosphorylation in muscle cells via PKC- and PKA-catalyzed pathways, as well as the identification of the phosphorylation target sites on AChR subunits. In addition, we investigated if changes in the association of surface AChR with the cytoskeletal framework modulated by these phosphorylation pathways contribute to the redistribution of surface AChR.

MATERIALS AND METHODS

Cell Culture and Drug Treatments. Primary cultures of skeletal muscle cells were prepared from 12 day chick embryos as previously described (*20*). Cells were plated on collagen-coated culture dishes at initial densities of 2.4×10^6 cells/60 mm culture dish, and grown in Dulbecco's modified Eagle's medium (DME) supplemented with 10% horse serum, and 2% embryo extract, at 37 °C in an atmosphere of 92% air, 8% CO_2. Under these conditions, myoblasts fused to form multinucleated myotubes on the second day after plating, and initiated rapid AChR synthesis on the third day. Where specified, embryonic chick brain extract (BE), prepared as described (*8*), was added to muscle cultures 4 days postplating to increase AChR clustering (*17*). Cultures were used 5 days after plating.

12-*O*-Tetradecanoylphorbol-13-acetate (TPA) was prepared as a 100 μg/mL stock in DMSO, and added directly to cultures at a final concentration of 100 nM. Okadaic acid (OA) was prepared as a 400 μM stock in DMSO, and used at a final concentration of 1 μM. Forskolin was prepared as a 10 mM stock in 95% ethanol, and added to cells at a final concentration of 100 μM. The equivalent concentrations of DMSO or ethanol added to control cultures had no effect on ^{32}P incorporation, AChR cluster stability, or AChR solubility in Triton X-100 extraction buffer. A stock of 0.1 M 8-bromo-cAMP was prepared in 20 mM Tris, pH 7.4, and added to cells at a final concentration of 0.5 mM.

Metabolic Labeling and Immunoprecipitation of AChR. Cell cultures were labeled with [^{32}P]orthophosphate (1 mCi/mL) in phosphate-free medium supplemented with 10% growth medium for 18 h, and the AChR-specific ligand ^{125}I-α-bungarotoxin (^{125}I-Bgt; 10 nM) was added for the final 1 h of incubation. Subsequent steps were carried out on ice. Labeling was terminated by two washes with DME, one wash with PBS, and a further wash with STE buffer (150 mM NaCl, 10 mM Tris, pH 7.4, 2 mM EGTA, 2 mM EDTA) containing protease inhibitors (5 mM benzamidine, 1 mM phenylmethylsulfonyl fluoride, 1% aprotinin, 10 μg/mL leupeptin, 10 mM *N*-ethylmaleimide) and phosphatase inhibitors (50 mM sodium fluoride, 40 mM sodium pyrophosphate, 20 mM potassium phosphate, 10 mM sodium molybdate, and 1 mM sodium orthovanadate). The cultures were then extracted for 30 min in STE buffer supplemented with 1% Triton X-100, a procedure that solubilizes total cellular AChR (*27*). Cell extracts were clarified by centrifugation for 30 min in the microfuge at 4 °C, and the supernatants were incubated with affinity-purified rabbit anti-α-Bgt antiserum for 3 h, and then with protein A−Sepharose beads for 1 h. The precipitates were washed 5 times with STE containing 1% Triton X-100, and suspended in 50 μL of SDS sample buffer (*28*). After incubation for 5 min in a boiling water bath, the beads were centrifuged, and the supernatants were fractionated on 10% SDS−polyacrylamide gels. The incorporation of [^{32}P]orthophosphate into AChR subunits was quantified using a phosphorimager.

In Vitro Phosphorylation of Immunoprecipitated AChR. To phosphorylate AChR in vitro with purified PKA or PKC, Bgt-labeled surface AChR was isolated from intact muscle cells by immunoprecipitation with anti-Bgt and protein A−Sepharose beads as described above, except that phosphatase inhibitors were omitted from the STE buffer. For PKC-catalyzed reactions, the precipitates were suspended in buffer containing [γ-^{32}P]ATP (30−50 μCi/100 μL reaction mixture), 20 mM HEPES, pH 7.4, 10 mM $MgCl_2$, 0.2 mM EGTA, 0.5 mM $CaCl_2$, 0.3 mM ATP, 10 μg of phosphatidylserine, 1 nM TPA, and purified PKC (Gibco, 0.5 unit). For PKA-catalyzed phosphorylation reactions, the buffer contained [γ-^{32}P]ATP (10−20 μCi/100 μL reaction mixture), 20 mM Tris, pH 7.4, 20 mM $MgCl_2$, 1 mM EDTA, 0.2% 2-mercaptoethanol, 0.3 mM ATP, and the PKA catalytic subunit (Sigma, 5 units). Incubations were for 1 h at 37 °C (PKC) or at 30 °C (PKA). The reactions were terminated by the addition of SDS sample buffer, and the proteins were fractionated by SDS−polyacrylamide gel electrophoresis. The ^{32}P-labeled protein bands were visualized by autoradiography.

Measurement of Stoichiometry of AChR Phosphorylation. To define the stoichiometry of surface AChR phosphorylation in intact muscle cells, the specific activity of [γ-^{32}P]ATP synthesized in [^{32}P]orthophosphate-labeled cultured chick myotubes was measured using a modification of published procedures (*29*, *30*). The [γ-^{32}P]ATP in cell extracts was quantified by measuring the ^{32}P incorporated into skeletal muscle phosphorylase *b* catalyzed by phosphorylase *b* kinase (Sigma). The phosphorylation of phosphorylase *b* was carried out in a reaction mixture containing 100 mM Tris, pH 8.0, 5 mM $MgCl_2$, 30 mM 2-mercaptoethanol, phosphorylase *b* (5 mg/mL), and cell extract from one 60 mm culture dish. After aliquots from the reaction mixture were fractionated by SDS−polyacrylamide gel electrophoresis, the protein band corresponding to phosphorylase *b* was visualized by Coomassie blue staining and excised from the gel, and the ^{32}P incorporation was quantified by liquid scintillation counting. The values obtained were compared to standards generated by incubations under identical conditions with 0.5 mM [γ-^{32}P]ATP of known specific activity instead of cell extract. Surface AChR was quantified by gamma counting of ^{125}I-Bgt, allowing the calculation of the molar ratio of phosphorylation of AChR subunits.

Fluorescence Microscopy. To visualize the cell surface distribution of AChR, myotubes grown on collagen-coated glass coverslips were labeled with 10 nM tetramethylrhodamine-conjugated Bgt (TMR-Bgt) for 1 h at 37 °C, rinsed with PBS, and fixed with 3.7% formaldehyde in PBS for 30 min at 4 °C. Fluorescence was examined with a Zeiss photomicroscope equipped with epi-illumination. For quan-

titation of clustering, under each assay condition clusters per myotube were counted in 50 randomly selected fields.

AChR Surface Labeling and Detergent Extraction. The anchorage of AChR to detergent-insoluble cytoskeletal frameworks was measured as described previously (*20*). Briefly, cultures labeled with 10 nM ^{125}I-Bgt were washed 5 times in PBS to remove unbound toxin, and then incubated for 3 min at room temperature with extraction buffer consisting of 0.3 M sucrose, 50 mM NaCl, 1 mM $MgCl_2$, 10 mM HEPES, pH 7.4, and 0.5% Triton X-100. After the extraction buffer containing the soluble protein fraction was removed, the remaining extraction-resistant fraction was dissolved in 1 N NaOH/1% Triton X-100. Both fractions were subjected to gamma counting, and the extracted AChR population was expressed as a percentage of the total amount of ^{125}I-Bgt bound to the cultures.

Expression and Purification of GST−δ Subunit Cytoplasmic Loop Fusion Protein. A glutathione-*S*-transferase (GST) fusion protein was constructed to incorporate a stretch of amino acids corresponding to the entire major cytoplasmic domain of chick AChR δ-subunit (*31*). A DNA fragment encoding amino acids 334 through 470 was prepared using PCR, ligated into the pGEX-2T vector between the unique endonuclease *Bam*H1 and *Eco*R1 sites, and introduced into *E. coli* by transformation. The solubilization and purification of the GST-fusion protein were performed by a modification of a published method (*32*). Cells were suspended in STE buffer containing 100 μg/mL lysozyme and incubated on ice for 15 min. Dithiothreitol (5 mM) and protease inhibitors (5 mM benzamidine, 1 mM phenylmethylsulfonyl fluoride, 10 mM *N*-ethylmaleimide) were added, and bacteria were lysed by sonication in the presence of 1.5% *N*-laurylsarcosine. The lysates were clarified by centrifugation, and the supernatants were adjusted to 4% Triton X-100 prior to incubation with glutathione−agarose beads for 30 min at 4 °C.

Phosphopeptide Mapping. Immunoprecipitated surface AChRs from ^{32}P-labeled myotube cultures or ^{32}P-labeled GST−δ fusion protein were fractionated on SDS−polyacrylamide gels, and proteins were transferred to nitrocellulose membranes. Labeled proteins were visualized by autoradiography, and the band corresponding to AChR δ-subunit or GST−δ fusion protein was excised and digested with *N*-tosyl-L-phenylalanine chloromethyl ketone (TPCK)-treated trypsin for 18 h in 50 mM ammonium bicarbonate, pH 8.0. After lyophilization, samples were subjected to two-dimensional phosphopeptide mapping as described by Boyle et al. (*33*). Briefly, the dried samples were dissolved in electrophoresis buffer, pH 1.9 (acetic acid:formic acid:water; 15.6:5:179.4), applied to a cellulose thin-layer chromatography (TLC) plate, and fractionated by electrophoresis in pH 1.9 buffer at 1.0 kV for 30 min using the Hunter peptide mapping system HTLE-7000. The plate was then air-dried, and peptides were separated in the second dimension by ascending chromatography in phosphochromatography buffer (glacial acetic acid:pyridine:1-butanol:water; 3:10:15:12) for 12 h. The plate was air-dried, and phosphopeptides were visualized by autoradiography.

Phosphoamino Acid Analysis. Phosphoamino acid analysis was performed by partial acid hydrolysis as described (*33*). Tryptic phosphopeptide samples were prepared as described above, and after lyophilization, the samples were resuspended in 6 N HCl and incubated for 60 min at 110 °C. After subsequent lyophilization, the samples were lyophilized again, and then resuspended in pH 1.9 electrophoresis buffer containing unlabeled phosphoamino acid standards (1 mg/mL each of phosphoserine, phosphothreonine, and phosphotyrosine in deionized water). This mixture was applied to TLC plates and separated by electrophoresis in pH 1.9 buffer for 20 min at 1.5 kV. After air-drying, the samples were subjected to second-dimension separation by electrophoresis in pH 3.5 buffer (glacial acetic acid:pyridine:water; 10:1:189) for 15 min at 1.3 kV. The TLC plates were air-dried, and the phosphoamino acids were visualized by autoradiography. To visualize the phosphoamino acid standards, the plates were sprayed with 0.25% ninhydrin in acetone and baked for 15 min at 65 °C.

Preparation of GST−δ Phosphopeptides for Microsequencing. Tryptic phosphopeptides derived from GST−δ fusion protein were subjected to amino acid sequence analysis by automated Edman degradation. Approximately 1 nmol of GST−δ fusion protein was phosphorylated by purified PKA or PKC in the presence of [γ-^{32}P]ATP, and the labeled protein was fractionated by SDS−PAGE and transferred to a nitrocellulose membrane before digestion by trypsin. The tryptic phosphopeptides were purified by passage through ferric chloride chelating columns (*34*), subsequently eluted from the column by NH_4HCO_3, pH 8.0, and purified further by reverse-phase HPLC on a C-18 column. The HPLC fractions were collected, and the radioactivity of each fraction was determined by Cerenkov counting. An aliquot of each ^{32}P-labeled HPLC fraction was subjected to two-dimensional phosphopeptide mapping, and GST−δ fusion protein phosphopeptides with migration patterns corresponding to those of phosphopeptides derived from in vivo phosphorylated AChR δ-subunit were subjected to microsequencing.

RESULTS

Characteristics of Cell Surface AChR Phosphorylation: Stoichiometry and Amino Acid Analysis. To assess the importance of AChR phosphorylation in the regulation of the surface distribution of these receptors, we first measured the stoichiometry of surface AChR phosphorylation in the intact muscle cells, i.e., the moles of phosphate incorporated per mole of surface AChR. Chick myotubes were incubated for 16 h with [^{32}P]orthophosphate, and cell surface AChR was then tagged with Bgt, extracted, and immunoprecipitated with anti-Bgt antibody. As can be seen in Figure 1A, surface AChR is phosphorylated on two of its subunits, the δ-subunit (M_r = 55K) and the γ-subunit (M_r = 50K), as we have identified earlier (*27*). ^{32}P labeling of AChR was quantitated by beta scanning of the dried SDS−polyacrylamide gels. To relate the radioactivity of phospholabeled AChR to the amount of phosphate bound to AChR subunits, the specific activity of the [γ-^{32}P]phosphate in the cellular ATP of the labeled cells was determined using published procedures (*29*, *30*) with modifications described under Materials and Methods. The amount of surface AChR was determined in replicate cultures by gamma counting of^{125}I-Bgt bound to immunoprecipitated AChR and comparing the counts to ^{125}I-Bgt standards of known molarity.

According to these measurements, the molar ratios of phosphate incorporated into AChR subunits under basal

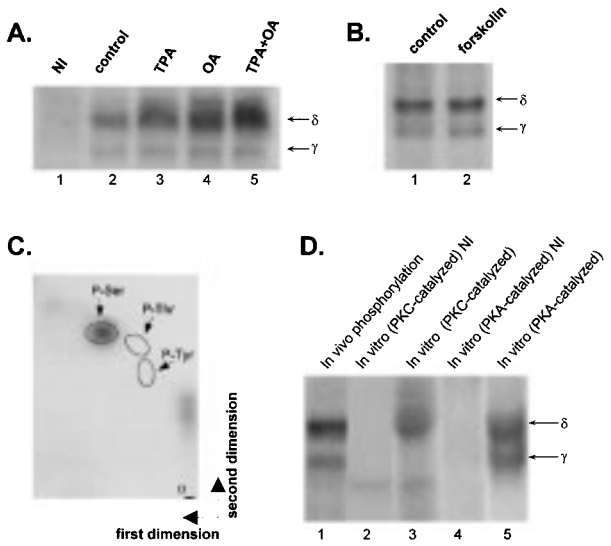

FIGURE 1: (A) Effects of TPA and OA on AChR phosphorylation. Cell cultures were labeled with [^{32}P]orthophosphate (1 mCi/mL) for 16 h and incubated with 10 nM ^{125}I-Bgt as well as 0.1 μM TPA and/or 1.0 μM OA for the final 1 h, and then rinsed and extracted as described under Materials and Methods. The extracts were immunoprecipitated with antisera against α-Bgt, and immunoprecipitates were resolved by SDS−polyacrylamide gel electrophoresis and autoradiography. Equal amounts of AChR, monitored by ^{125}I-Bgt gamma counting, were loaded onto each lane. Lane 1, nonimmune; lane 2, untreated control; lane 3, TPA-treated; lane 4, OA-treated; lane 5, TPA- and OA-treated. Positions of AChR γ- and δ-subunits are shown by arrows on the right. (B) Effects of forskolin on AChR phosphorylation. Cell cultures labeled with [^{32}P]-orthophosphate as above, were treated with 0.1 mM forskolin during ^{125}I-Bgt labeling, then extracted, immunoprecipitated, and resolved by SDS−polyacrylamide gel electrophoresis as above. Lane 1, untreated control. Lane 2, forskolin-treated. (C) Phosphoamino acid analysis of ^{32}P-labeled AChR δ-subunit. Cell cultures were labeled with [^{32}P]orthophosphate and ^{125}I-Bgt, then extracted, immunoprecipitated, resolved by SDS−polyacrylamide gel electrophoresis, and transferred to a nitrocellulose membrane. Phosphoamino acid analysis was carried out as described under Materials and Methods. The migration patterns of P-Ser, P-Thr, and P-Tyr, as identified by ninhydrin staining of phosphoamino acid standards, are indicated by open ellipses. The origin located at the bottom right is marked by an open circle. The directions of the electric fields during electrophoreses are indicated by the arrows. (D) In vitro phosphorylation of AChR subunits by purified PKC and PKA. Myotube cultures were labeled with 10 nM ^{125}I-Bgt for 1 h, and surface AChR was immunoprecipitated with anti-Bgt antibody as described under Materials and Methods. Phosphorylation reactions of immunoprecipitated AChR with [γ-^{32}P]ATP and purified PKC or PKA were carried out as detailed under Materials and Methods. Phosphorylated AChR subunits were resolved by SDS−polyacrylamide gel electrophoresis and autoradiography. Lane 1 in vivo phosphorylated AChR, γ- and δ-subunits immunoprecipitated from ^{32}P-labeled cultured chick myotubes, included as standards to show migration positions of these subunits. Lane 2, PKC-catalyzed in vitro phosphorylation of nonimmune control. Lane 3, PKC-catalyzed in vitro phosphorylation. Lane 4, PKA-catalyzed in vitro phosphorylation of nonimmune control. Lane 5, PKA-catalyzed in vitro phosphorylation.

conditions are approximately 1.4 (1.42 ± 0.09) mol/mol of δ-subunit and 0.3 (0.36 ± 0.05) mol/mol of γ-subunit. (Data are means ± SD from six independent determinations.) This stoichiometry suggests that, assuming the availability of three phosphorylation sites on the AChR δ-subunit in cultured myotubes (*35*), between 40% and 100% of surface AChR is phosphorylated under basal conditions. The relatively high proportion of surface AChRs that are phosphorylated is consistent with the possibility that phosphorylation plays a significant role in the regulation of surface AChR distribution.

To identify the phosphorylated amino acid residues on subunits of AChR immunoprecipitated from the surface of intact myotubes, two-dimensional phosphoamino acid analysis was performed. As shown in Figure 1C, AChR δ-subunit under these conditions is phosphorylated exclusively on serine residues. Similarly, δ-subunit phosphorylated in TPA- or OA-treated cells, as well as the γ-subunit, was found to be labeled exclusively on serines (not shown).

Effects of Pharmacological Agents on AChR Phosphorylation. To investigate the contribution of PKC, PKA, and phosphoprotein phosphatases to the phosphorylation state of AChR in intact muscle cells, we used pharmacological activators of PKC and PKA as well as an inhibitor of phosphoprotein phosphatases PP-1 and PP-2A. Exposure of intact myotubes for 1 h to the PKC activator TPA (0.1 μM) was seen to cause a marked increase in the phosphorylation of the δ-subunit, whereas no change was detected in the phosphorylation of the γ-subunit under these conditions (Figure 1A, compare lanes 2 and 3). This result is consistent with the presence of a previously identified conserved phosphorylation site for PKC in the major cytoplasmic loop of *Torpedo* AChR δ-subunit but not of the γ-subunit (*35*). In contrast, despite the presence of consensus sequences for PKA phosphorylation on both the δ- and γ-subunits (*35*), treatment of these cells with the PKA activator forskolin (Figure 1B), or with the cell-permeable cAMP analogue 8-bromo-cAMP, did not alter the phosphorylation state of surface AChR (not shown).

Treatment of the myotubes with OA (1.0 μM), a potent inhibitor of the phosphoprotein phosphatases PP-1 and -2A, caused a significant increase in the net phosphorylation of both subunits (Figure 1A, lane 4). Moreover, when myotubes were exposed to TPA and OA together, the effects appeared to be additive. In the representative experiment shown in Figure 1A, combined treatment of myotubes with TPA and OA stimulated phosphorylation of the δ-subunit by 1.8-fold, while either agent alone caused stimulation of 1.5-fold (TPA) and 1.6-fold (OA), as quantified using a Phosphorimager. Thus, as calculated from the molar ratio of AChR phosphorylation under basal conditions, in the presence of either TPA or OA alone the stoichiometry of AChR phosphorylation is increased to 2−2.3 mol of phosphate/mol of AChR δ-subunit, while in the presence of both of these agents, 2.3−2.7 mol of phosphate is incorporated per mole of AChR δ-subunit. The latter stoichiometry approaches the saturation level for incorporation of phosphate by the δ-subunit, assuming that three phosphorylation sites are available.

In Vitro Phosphorylation of AChR by Purified PKC and PKA. To examine whether AChR γ- and δ-subunits are direct substrates for PKC- and PKA-catalyzed phosphorylations, we carried out phosphorylation of AChR in vitro with purified PKC and PKA. AChR on the surface of intact chick myotubes was labeled with Bgt and subsequently isolated from the cell extracts by immunoprecipitation with anti-Bgt antiserum, as described under Materials and Methods. The immunoprecipitated AChR conjugated to protein A−Sepharose beads was then phosphorylated by purified PKC or PKA in the presence of [γ-^{32}P]ATP. The products

of the phosphorylation reaction were fractionated by SDS−polyacrylamide gel electrophoresis, and ^{32}P-labeled subunits were visualized by autoradiography.

In Figure 1D, lane 1, in vivo phosphorylated AChR was isolated from ^{32}P-labeled cell cultures by immunoprecipitation with anti-Bgt and fractionated by SDS−polyacrylamide gel electrophoresis to mark the migration patterns of the γ- and δ-subunits. Figure 1D (lanes 2−5) shows the fractionation patterns of immunoprecipitated Bgt−AChR complexes that were phosphorylated in vitro with purified PKC (lane 3) or PKA (lane 5), as compared with the corresponding nonimmune controls (lanes 2, 4). As can be seen, only the δ-subunit is phosphorylated by purified PKC (lane 3), whereas both the γ- and δ-subunits are phosphorylated by purified PKA (lane 5). To test the possibility that the lack of γ-subunit phosphorylation by PKC was due to preexistent phosphorylation, we pretreated the immunoprecipitates with potato acid phosphatase. This treatment had no effect on the phosphorylation pattern (A.S.N. and J.M.P., unpublished data). These results show that chick AChR δ-subunits contain substrate sites for both PKA- and PKC-catalyzed phosphorylation while γ-subunits are phosphorylated by PKA and not by PKC.

Effects of TPA and OA on AChR Surface Distribution. To determine if the increases in AChR phosphorylation induced by OA are accompanied by changes in AChR surface distribution similar to the cluster dispersal seen upon treatment of muscle cells with TPA (*17, 18*), cultured chick myotubes were exposed to 1 μM OA for 1 h, and surface AChR was visualized by labeling the cells with TMR-Bgt. Displayed in Figure 2, panels A and B, are similar fields showing myotubes before and after OA treatment. As can be seen, a 1 h exposure to OA produces a substantial reduction in the number of clusters. Panels C and D of Figure 2 are higher magnification views of single myotubes illustrating that the AChR cluster dispersal by OA is associated with increased AChR staining in the surrounding areas. This increase in diffuse AChR staining reflects the lateral dispersal of AChR from clusters into adjacent regions of the muscle cell membrane. As monitored by ^{125}I-Bgt binding experiments, OA-induced AChR declustering is not accompanied by a decrease in the surface levels of AChR (not shown). In this respect, the effect of OA on AChR cluster stability resembles the declustering induced by TPA that was reported earlier (*17*). In contrast to the marked decrease in the number of clusters caused by the 1 h exposure to OA, there was no appreciable change in myotube morphology. However, some morphological effects similar to those obtained with TPA, a tendency of some of the myotubes to round into a more cylindrical shape, were evident at longer times of exposure (2−3 h; not shown). Thus, declustering of surface AChR was not accompanied by the loss of cells, a decrease in surface AChR levels, or signs of general toxicity. In control experiments, the treatment of cultures for 3 h with 1-norokadaone (1 μM), a structural analogue with similar physical and chemical properties as okadaic acid but lacking phosphatase inhibitory activity, did not induce either the declustering of surface AChR or the change in cell shape (not shown).

Furthermore, like the effects of these agents on AChR phosphorylation, the actions of OA and TPA on cluster stability are additive. As quantified in Figure 2E by counting

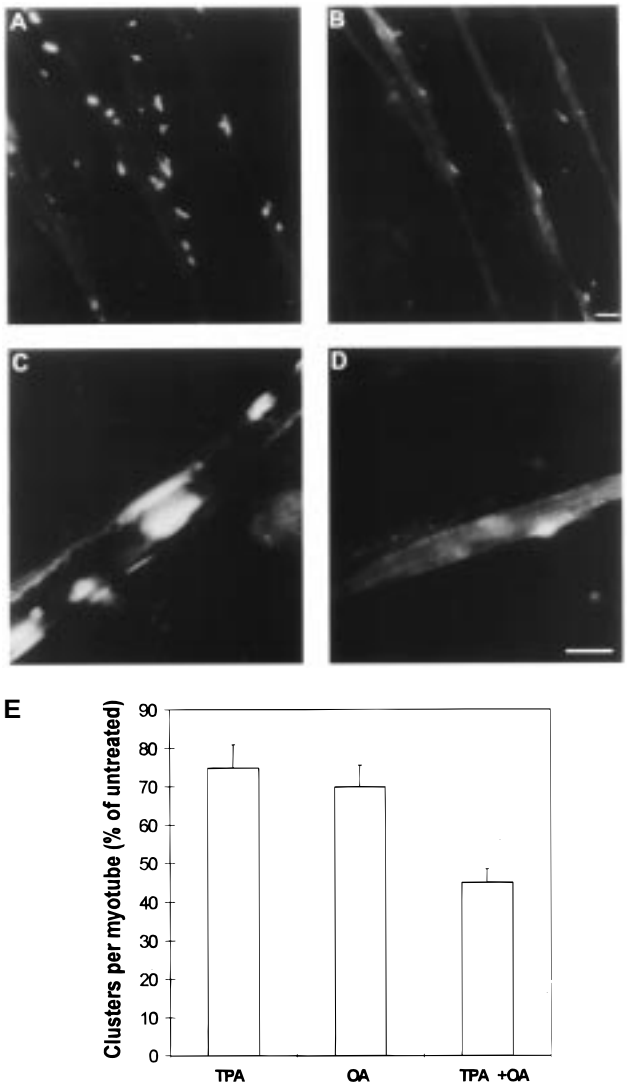

FIGURE 2: Effect of OA on the distribution of AChR on the surface of cultured muscle cells. Five-day-old chick myotube cultures on glass coverslips were pretreated with BE for 1 day to promote AChR clustering, and then exposed to 1 μM OA and 10 nM TMR-α-Bgt for 1 h. Cells were fixed and prepared for fluorescence microscopy as described under Materials and Methods. (A and B) Low magnification fluorescent image of untreated (A) and OA-treated (B) myotubes. Note the decrease in number of AChR clusters. Bar, 50 μm. (C and D) Higher magnification fluorescent image of untreated (C) and OA-treated (D) myotube. Bar, 10 μm. Note the decrease in AChR clusters and the increase in diffuse staining. (E) The loss of AChR clusters induced by treatment with TPA, OA, and TPA plus OA, as quantified by counting the number of clusters per myotube in 50 randomly selected fields and averaged among triplicate determinations. Data shown represent the mean of five independent experiments ± SD.

the number of clusters per myotube in 50 randomly selected fields, we observed that a 1 h exposure to either 0.1 μM TPA or 1 μM OA resulted in a 25−30% decrease in the number of clusters, while addition of both agents together induced a decrease of approximately 50% in the number of AChR clusters per myotube [clusters per myotube ± SD: controls, 5.2 ± 0.8; TPA-treated, 3.8 ± 0.5; OA-treated, 3.6 ± 0.6; TPA + OA, 2.5 ± 0.5 (n = 5)].

OA and TPA Increase the Triton X-100 Extractability of Surface AChR. Mild detergent treatment of cultured muscle results in the extraction of the membrane lipid bilayer along with soluble proteins and dispersed surface AChR: in

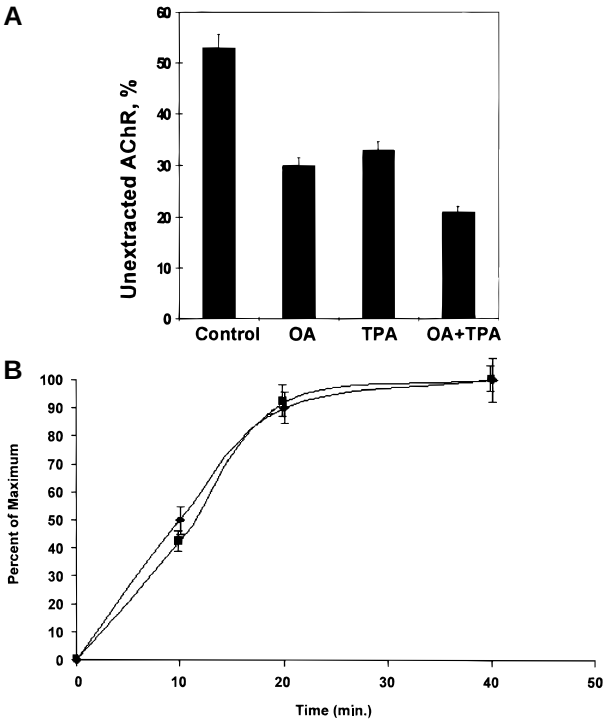

FIGURE 3: (A) Effects of TPA and OA on the extractability of AChR by Triton X-100. Cell cultures were labeled with 10 nM ^{125}I-Bgt for 1 h, and then incubated with 0.1 μM TPA and/or 1.0 μM OA for 1 h. Cells were subsequently treated for 3 min with extraction buffer containing 0.5% Triton X-100 and then extracted. ^{125}I-Bgt−AChR complexes were quantified by gamma counting. The remaining AChR was solubilized by 30 min treatment with 1 M NaOH containing 1% Triton X-100 and quantified by gamma counting. In each case, the percentage of total AChR that was retained on myotubes is expressed as the mean of four determinations ± SD. (B) Comparison of time courses of the effects of TPA on AChR δ-subunit phosphorylation (◆) and on the extractability of AChR by Triton X-100 (■). Cell cultures, labeled with [^{32}P]-orthophosphate as above, were treated with 0.1 μM TPA for the intervals specified, then Bgt-labeled, extracted, and immunoprecipitated with anti-Bgt as above. [^{32}P]Orthophosphate incorporation into the δ-subunit was quantified by Phosphorimager. Companion cultures were labeled with 10 nM ^{125}I-Bgt for 1 h, and then incubated with 0.1 μM TPA for the specified intervals. Cells were subsequently treated for 3 min with extraction buffer containing 0.5% Triton X-100, and the proportion of total ^{125}I-α-Bgt−AChR labeling that was extracted by detergent was quantified by gamma counting. Results are expressed as the percentage of total AChR that was extracted. Each point represents the mean of four determinations; error bars = SD.

contrast, clustered AChR was shown to be resistant to detergent extraction and remains associated with the detergent-insoluble cytoskeletal framework (*20*, *22*, *36*). In addition, in comparison to diffusely distributed AChR, the resistance of clustered AChR to detergent extraction is associated with decreased lateral mobility of clustered receptors in the plane of the membrane (*21*, *26*). To define the relationship between AChR phosphorylation on Ser residues and declustering, we have investigated the effects of TPA and OA on the detergent extractability of surface AChR.

Cultured myotubes 5 days after plating were labeled with ^{125}I-Bgt for 1 h and then treated with OA (1 μM), TPA (0.1 μM), or both, for an additional 1 h. Cultures were then subjected to mild detergent extraction in buffer containing 0.5% Triton X-100 for 3 min. As shown in Figure 3, in the absence of drug treatment slightly over 50% of the total surface AChR remained associated with the detergent-insoluble cytoskeleton after 3 min of extraction. Exposure of the myotubes to either OA or TPA produced roughly equivalent increases in AChR extractability, reducing the fraction of surface AChR that remained unextracted to approximately 30% of total AChR, while combined treatment with both agents further decreased the fraction of unextracted AChR to about 20%. It is noteworthy that this additive effect of OA and TPA on AChR detergent extractability parallels the additive action of these drugs on the extent of AChR δ-subunit phosphorylation. Moreover, the effects of TPA on AChR phosphorylation levels and extractability showed a similar time course, reaching maximal levels by 20 min of exposure of cells to the phorbol ester (Figure 3B). These results suggest that increased net phosphorylation of AChR mediated by PKC activation or phosphoprotein phosphatase inhibition weakens the interaction between surface AChR and the cytoskeleton, resulting in an increase of AChR lateral mobility and declustering.

Phosphopeptide Mapping of AChR δ-Subunit. To locate the sites on the δ-subunit of muscle cell surface AChR that are the targets of TPA- and OA-enhanced phosphorylation, two-dimensional phosphopeptide analysis was carried out. In these experiments, Bgt−AChR complexes were immunoprecipitated from ^{32}P-labeled myotube cultures using anti-Bgt antisera, the immunoprecipitates were fractionated on SDS−polyacrylamide gels, and the fractionated proteins were transferred to nitrocellulose membranes. The band corresponding to AChR δ-subunit was excised and subjected to digestion with TPCK−trypsin, and the resulting phosphopeptides were separated in two dimensions. AChR δ-subunit from cells labeled with [^{32}P]orthophosphate was found to contain three major tryptic phosphopeptides, designated as *a*, *b*, and *c* (Figure 4). Comparison of the phosphopeptide maps derived from untreated control cells with those from TPA-treated cells (Figures 4, compare panels 1 and 2) shows that while TPA treatment did not change this phosphopeptide pattern, phosphorylation of each of the three peptides was markedly increased, most clearly in the case of peptide *a*. These results suggest that all three tryptic peptides contain sites that are targets for PKC-catalyzed phosphorylation.

As shown in Figure 4, panel 3, the enhanced AChR δ-subunit phosphorylation induced by OA is reflected by increases in phosphorylation of tryptic phosphopeptides *a* and *c*, indicating that these peptides contain active target sites for PKC and phosphatases 1 and/or 2a and undergo continuous phosphorylation/dephosphorylation. Supporting this suggestion is the result shown in Figure 4, panel 4, showing that treatment of the cells with OA together with TPA enhanced the levels of phosphorylation of both peptides *a* and *c* to a greater extent than either treatment alone.

Phosphopeptide Mapping of GST−δ Fusion Protein. To precisely identify the phosphorylation sites on the AChR δ-subunit, we designed a GST−δ fusion protein containing the entire major cytoplasmic loop (amino acids 311−447) of chick AChR δ-subunit, where all of the putative phosphorylation sites are thought to be located (*35*). The strategy was to compare tryptic phosphopeptide maps obtained from surface AChR in intact muscle cells with those generated by phosphorylation with purified PKC and PKA and tryptic digestion of this GST−δ fusion protein. Upon identification of phosphopeptides with the same migration patterns, the

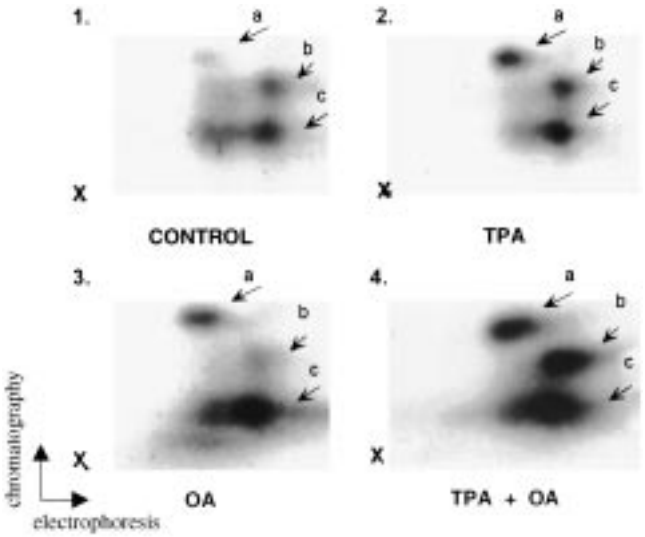

FIGURE 4: Phosphopeptide mapping of ^{32}P-labeled AChR δ-subunit. Cell cultures were labeled with [^{32}P]orthophosphate for 16 h, and 0.1 μM TPA or 1.0 μM OA, or both, as well as 10 nM ^{125}I-α-Bgt were added to cultures during the final 1 h of incubation. AChR was isolated by immunoprecipitation with anti-Bgt antiserum, immunoprecipitates were fractionated by SDS−polyacrylamide gel electrophoresis and transferred to a nitrocellulose membrane, and the protein band corresponding to AChR δ-subunit was excised and digested by trypsin. The tryptic phosphopeptides were separated by electrophoresis in the first dimension and ascending chromatography in the second dimension as described under Materials and Methods. The individual phosphopeptides were visualized by autoradiography. Panels 1−4 show phosphopeptide maps of ^{32}P-labeled AChR δ-subunit derived from untreated cells (panel 1), TPA-treated cells (panel 2), OA-treated cells (panel 3), and TPA + OA-treated cells (panel 4). The origin is indicated at the bottom left of each panel. The directions of the separations in both dimensions are indicated by large arrows, and the individual phosphopeptides are marked by small arrows.

GST−δ phosphopeptides could then be sequenced to identify the corresponding phosphorylation sites on the AChR δ-subunit.

Phosphorylation of the GST−δ fusion protein catalyzed by either PKC or PKA was carried out in the presence of [γ-^{32}P]ATP as described under Materials and Methods. Figure 5, panel 2 is a map of tryptic phosphopeptides derived from GST−δ phosphorylated in vitro by purified PKC. Three phosphopeptides derived from PKC-phosphorylated GST−δ, designated as *x*, *y*, and *z*, were seen to migrate with the same pattern as phosphopeptides *a*, *b*, and *c* from the in vivo phosphorylated AChR δ-subunit. To confirm that peptides *a* and *x*; *b* and *y*; and *c* and *z* are identical, these phosphopeptides were recovered from the TLC plates, mixed pairwise, and reseparated in two dimensions. Figure 5 (panels 4−7) shows that the peptide mixtures *a* + *x; b* + *y*; and *c* + *z* comigrated in all cases, consistent with the interpretation that these peptides are identical.

Although in our experiments PKA activators failed to induce increased AChR δ-subunit phosphorylation in intact cells, we observed that PKA catalyzes the phosphorylation of immunoprecipitated AChRδ-subunit in vitro (see Figure 1D). To locate the PKA-catalyzed phosphorylation site(s), the GST−δ fusion protein was phosphorylated in vitro by purified PKA in the presence of [γ-^{32}P]ATP. Figure 5, panel 3 shows that one of the tryptic phosphopeptides derived from GST−δ was labeled by the PKA-catalyzed phosphorylation. This peptide, designated as peptide *w*, was found to comigrate with peptide *a* derived from an in vivo phosphorylated AChR δ-subunit: furthermore, mixing experiments (Figure 5, panel 7) showed that these two peptides are identical. Thus, a PKA target site that is phosphorylated in vitro is located in the same tryptic peptide of the AChR δ-subunit as one of the PKC target sites.

These findings show, first, that all the sites on AChR δ-subunit that are phosphorylated in intact cells are located in the major cytoplasmic loop. Second, all three AChR tryptic phosphopeptides are targets for PKC phosphorylation, and one of these peptides is also phosphorylated by purified PKA. Finally, phosphorylation of all three phosphopeptides is stimulated by the pharmacological activation of PKC by TPA in intact muscle cells. In contrast, pharmacological activators of PKA did not enhance the phosphorylation of surface AChR in intact chick muscle cells.

Identification of Phosphorylation Sites. We identified the phosphorylation sites on AChR δ-subunit utilizing the tryptic phosphopeptides generated from the GST−δ fusion protein as described under Materials and Methods. The phosphopeptides corresponding to peptides *x*, *y*, and *z* were subjected to amino acid sequence analysis by Edman degradation utilizing an automated microsequencer. This analysis identified the amino acid sequence of peptide *x* to be Arg-Cys-Ser-Ser-Ala-Gly-Tyr-Ilu-Ala-Lys, which corresponds exactly to the sequence Arg^{375} through Lys^{384} of the AChR δ-subunit (Figure 6). The phosphorylated residue within this peptide was identified by radioactive microsequencing as Ser^{378}. This site is consistent with a proposed consensus sequence for PKC-mediated phosphorylation, Arg-X-X-Ser (*37*, *38*). Amino acid sequence analysis of peptide *y* established that it corresponds to the sequence Asn^{449}-Ser-Tyr-Asn-Glu-Glu-Lys-Asp-Asn-Trp-Asn-Arg^{460} of AChR δ-subunit. In this peptide, the Lys−Asp bond was not cleaved by trypsin, consistent with the suggestion that trypsin does not efficiently cleave between these amino acids (*33*). This phosphopeptide contains only one serine residue, and the radiosequence analysis confirmed that the second residue of this peptide (Ser^{450}) was phosphorylated.

Amino acid sequence analysis of peptide *z* revealed the peptide sequence to be Ala-Glu-Glu-Tyr-Tyr-Ser-Val-Lys-Ser-Arg, identical to the peptide sequence Ala^{385}−Arg^{394} on the AChR δ-subunit. Radiosequence analysis identified the phosphorylated residue at the ninth position which corresponded to the Ser^{393}. This site has been previously suggested to be a potential target for PKC-catalyzed phosphorylation since it is flanked by the basic residues Lys and Arg, characteristic of other known substrates for PKC (*35*, *37*).

Identification of the PKA-catalyzed phosphorylation site of GST−δ was carried out similarly to the identification of PKC-catalyzed phosphorylation sites. Amino acid sequence analysis demonstrated that the phosphopeptide substrate of PKA is Arg-Cys-Ser-Ser-Ala-Gly-Tyr-Ile-Ala-Lys, identical to peptide *x* which was shown above to undergo PKC-mediated phosphorylation. Radiosequencing of this phosphopeptide demonstrated that Ser^{377} was phosphorylated by PKA. This identification is consistent with the previously suggested consensus sequence for PKA: Arg-Arg-X-Ser (*39*).

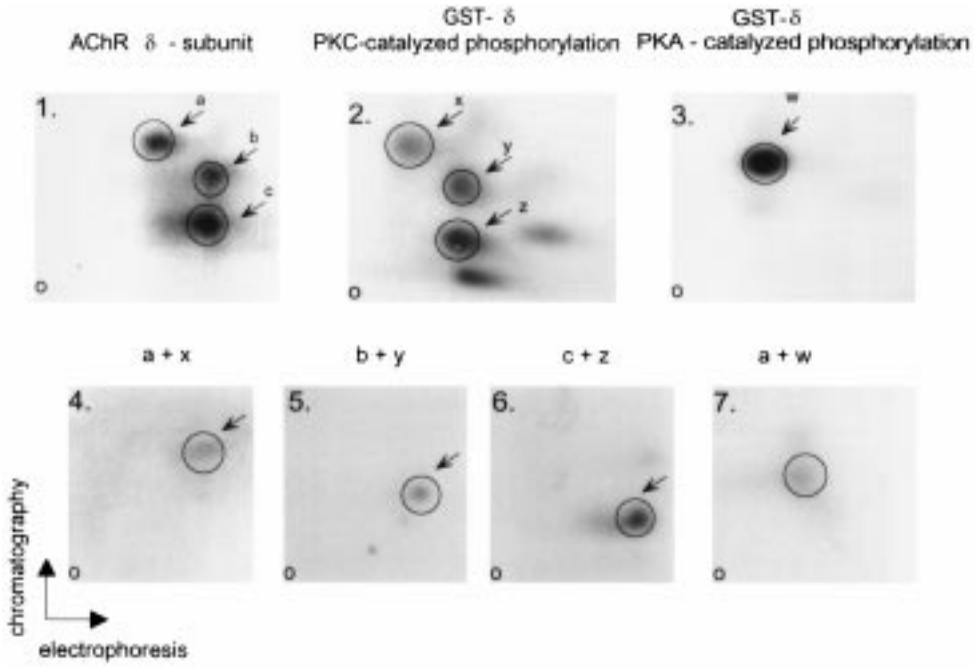

FIGURE 5: Phosphopeptide mapping of PKC- and PKA-catalyzed phosphorylated GST−δ fusion protein. In vitro phosphorylation of GST−δ fusion protein by purified PKC or PKA and phosphopeptide mapping were carried out as described under Materials and Methods. Panels are as follows: 1, phosphopeptide pattern of AChR δ-subunit derived from in vivo phosphorylated surface AChR in TPA-treated cultures; 2, phosphopeptide pattern of GST−δ phosphorylated by purified PKC; 3, phosphopeptide pattern of GST−δ phosphorylated by purified PKA. To establish the identity of individual phosphopeptides, these were recovered from TLC plates and eluted, and the samples containing equivalent radioactivity of peptides *a* and *x* (panel 4), *b* and *y* (panel 5), *c* and *z* (panel 6), and *a* and *w* (panel 7) were mixed and reseparated in two dimensions.

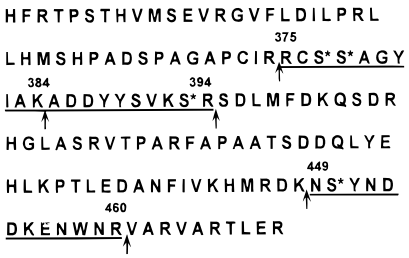

FIGURE 6: The amino acid sequence of the major cytoplasmic domain of AChR δ-subunit. The amino acid sequence between residues 358 and 470 of chick AChR δ-subunit is shown. The phosphopeptides generated by tryptic digestion are underlined. The arrows indicate tryptic cleavage sites. Asterisks mark phosphorylation sites on Ser^{377}, Ser^{378}, Ser^{393}, and Ser^{450} as revealed by microsequencing.

DISCUSSION

In the present study, we have determined that the PKC-catalyzed phosphorylation of AChR on the surface of cultured chick muscle cells is directed to one or more of three serines (Ser^{378}, Ser^{393}, Ser^{450}) located in the major intracellular domain of AChR δ-subunit. In addition, exposure of myotubes to OA produced elevated phosphorylation on Ser^{378} and Ser^{450}. Phosphorylation at these sites was accompanied by the dispersal of AChR clusters and the decreased association of AChR with the detergent-resistant cytoskeletal framework.

These findings are consistent with the possibility that increased phosphorylation of AChR on Ser residues in the major cytoplasmic domain promotes detachment of AChR from their anchorage to structural proteins which constrain the lateral mobility of clustered AChR. Thus, the present results suggest a molecular mechanism for the dispersal of AChR clusters by TPA reported earlier by ourselves (*17*) and others (*18*). Conversely, increased phosphorylation of AChR on Tyr residues has been reported to be associated with the formation of AChR clusters induced by the neural clustering protein agrin (*12*−*15*, *26*). As has been demonstrated in nerve−muscle co-cultures, the accumulation of AChR beneath the nerve terminal is accompanied by the dispersal of AChR clusters from extrasynaptic regions (*3*). Thus, the redistribution of AChRs during synaptogenesis can be regulated by the simultaneous activation of these two kinase pathways, resulting in the spatially coordinated dispersal and aggregation of preexistent surface AChR.

How might increased AChR phosphorylation lead to the redistribution of surface AChR? AChR at cluster sites appears to be selectively anchored to subjacent cytoskeletal elements (*19*, *40*), as evidenced by its resistance to detergent extraction (*20*) and restricted lateral mobility in the plane of the membrane (*21*). Recent findings show that the induction of AChR clustering by agrin involves increased resistance of these receptors to detergent extraction (*18*, *26*), accompanied by increased phosphorylation on Tyr residues (*15*, *26*). Mechanistically, AChR attachment to the structural framework may be mediated by specific motifs on cytoskeleton-associated proteins that selectively bind phosphotyrosine, such as SH2 and PTB domains (*41*−*43*). In contrast, phosphorylation on Ser and Thr residues may serve to disrupt protein−protein interactions (*44*). Our present findings that TPA and OA cause AChR declustering as well as increased detergent extractability suggest that increased AChR phosphorylation on Ser residues weakens its anchorage to the underlying cytoskeleton, resulting in the destabilization of AChR clusters. It should be noted that aside from the direct effects on AChR phosphorylation, TPA and OA also cause

increased phosphorylation of other cellular proteins: thus, it remains possible that the AChR cluster dispersal induced by these agents is a consequence of the increased phosphorylation of as yet unidentified target proteins that are involved in receptor anchorage to the cytoskeletal framework.

We have found that the δ-subunit of chick AChR in intact muscle cells is phosphorylated at three distinct sites: Ser^{378}, Ser^{393}, and Ser^{450}, all of which are target sites for PKC. Ser^{378} is located within the tryptic phosphopeptide Arg^{375}-Cys-Ser-Ser-Ala-Gly-Tyr-Ilu-Ala-Lys^{384} which also contains a consensus target site for PKA (Ser^{377}) that is immediately adjacent to the PKC site (*31*, *35*). Moreover, we have found that this site was efficiently phosphorylated by purified PKA in vitro. Previously, the corresponding stretch of amino acids in *Torpedo* AChR δ-subunit was reported to be phosphorylated both by PKA and by PKC (*45*). Unexpectedly, in our in vivo experiments, treatment of chick muscle cells with either of two PKA activators, forskolin and 8-bromo-cAMP, had no effect on the phosphorylation of AChR δ-subunit, suggesting that PKA does not actively phosphorylate the δ-subunit in intact chick muscle cells. In contrast, AChR δ-subunit phosphorylation by PKA has previously been observed in mouse BC3H1 myocytes (*30*) as well as in rat myotubes (*46*, *47*). Interspecies differences in AChR phosphorylation patterns have been documented (*48*, *49*), and in the case of Ser^{377} of AChR δ-subunit in intact chick myotubes, one possibility is that the native conformation of AChR may render this site inaccessible to PKA, as has been documented in other instances (*50*). Alternatively, it is possible that the phosphorylation catalyzed by PKC of Ser^{378} may prevent the PKA-catalyzed phosphorylation at Ser^{377} in the chick muscle cells. A third possibility, that the lack of effect of forskolin on δ-subunit labeling could be due to the stable phosphorylation of the PKA target sites in vivo prior to ^{32}P labeling, is unlikely since prior phosphorylation of immunopurified δ-subunit was not detected by comparison of in vitro ^{32}P labeling levels with and without potato phosphatase pretreatment (A.S.N. and J.M.P., unpublished data).

A second PKC site identified in the present study is Ser^{393}, which is situated between Lys and Arg residues and is conserved between species (*35*). The homologous site in *Torpedo* AChR δ-subunit has been reported to undergo PKC-catalyzed phosphorylation in vitro (*51*). Moreover, it has been shown that Ser^{362} and Ser^{377} in *Torpedo* δ-subunit, corresponding to Ser^{378} and $Ser^{393}$of chick δ-subunit, both contained phosphate groups upon the purification of AChR from *Torpedo californica* electric tissue (*52*). This finding suggested that, as in the present case of cultured chick myotubes, the homologous sites in *Torpedo* are also phosphorylated in vivo. However, the *Torpedo* phosphorylation is highly stable, surviving the extensive purification steps even in the absence of protein phosphatase inhibitors (*52*). In contrast, the phosphorylation of these serines in chick muscle AChR is highly transient, as shown by our observation that the inhibition of phosphoprotein phosphatases by OA causes a rapid, significant increase in net ^{32}P-labeling at these residues. A third, novel phosphorylation site, Ser^{450}, was found in the present study to undergo TPA-dependent phosphorylation in vivo and PKC-catalyzed phosphorylation in vitro. Thus, of the 3 PKC phosphorylation sites on chick AChR δ-subunit, all are located within the major cytoplasmic loop, 2 are situated within a 15 amino acid stretch, and 1 site is found significantly further along the length of the cytoplasmic loop, close to the fourth transmembrane span. It is possible, however, that this third phosphorylation site is situated in close proximity to the other two sites in the native conformation of the δ-subunit, and that phosphorylation at these sites mediates the detachment of clustered AChR from the underlying cytoskeleton.

ACKNOWLEDGMENT

We thank Barry Yee, Nazneen Rahman, and Sandeep Mody for expert technical assistance.

REFERENCES

1. Hall, Z. W., and Sanes, J. R. (1993) *Cell 71/Neuron 10 (Suppl.)*, 99−121.
2. Anderson, M. J., and Cohen, M. W. (1977) *J. Physiol. 268*, 757−773.
3. Moody-Corbett, F., and Cohen, M. W. (1982) *J. Neurosci. 2*, 633−646.
4. McMahan, U. J. (1990) *Cold Spring Harbor Symp. Quant. Biol. 55*, 407−418.
5. Bowe, M. A., and Fallon, J. R. (1995) *Annu. Rev. Neurosci. 18*, 443−462.
6. Christian, C. N., Daniels, M. P., Sugiyama, H., Vogel, Z., Jacques, L., and Nelson, P. J. (1978) *Proc. Natl. Acad. Sci. U.S.A. 75*, 4011−4015.
7. Podleski, T. R., Axelrod, D., Ravdin, P., Greenberg, I., Johnson, M. M., and Salpeter, M. M. (1978) *Proc. Natl. Acad. Sci. U.S.A. 74*, 2035−2039.
8. Jessel, T. M., Seigel, R. E., and Fischbach, G. D. (1979) *Proc. Natl. Acad. Sci. U.S.A. 76*, 5397−5401.
9. Nitkin, R. M., Smith, M. A., Magill, C., Fallon, J. R., Yoa, Y.-M. M., Wallace, B. G., and McMahan, U. J. (1987) *J. Cell Biol. 105*, 2471−2478.
10. DeChiara, T. M., Bowen, D. C., Valenzuela, D. M., Simmons, M. V., Poueymirou, W. T., Thomas, S., Kinetz, E., Compton, D. L., Rojas, E., Park, J. S., Smith, C., DiStefano, P. S., Glass, D. J., Burden, S. J., and Yancopoulos, G. D. (1996) *Cell 45*, 501−512.
11. Glass, D. J., Bowen, D. C., Stitt, T. N., Radziejewski, C., Bruno, J., Ryan, T. E., Gies, G. R., Shah, S., Mattson, K., Burden, S. J., DiStefano, P. S., Valenzuela, D. M., DeChiara, T. M., and Yancopoulos, G. D. (1996) *Cell 45*, 513−524.
12. Wallace, B. G., Qu, Z., and Huganir, R. L. (1991) *Neuron 6*, 869−878.
13. Qu, Z., and Huganir, R. L. (1994) *J. Neurosci. 14*, 6834−6841.
14. Wallace, B. G. (1995) *J. Cell Biol. 128*, 1121−1129.
15. Ferns, M., Deiner, M., and Hall, C. (1996) *J. Cell Biol. 132*, 937−944.
16. Wallace, B. G. (1994) *J. Cell Biol. 125*, 661−668.
17. Ross, A., Rapuano, M., and Prives, J. (1988) *J. Cell Biol. 107*, 1139−1145.
18. Wallace, B. G. (1988) *J. Cell Biol. 107*, 267−278.
19. Froehner, S. C. (1991) *J. Cell Biol. 114*, 1−7.
20. Prives, J., Fulton, A. B., Penman, S., Daniels, M. P., and Christian, C. N. (1982) *J. Cell Biol. 92*, 231−236.
21. Stya, M., and Axelrod, D. (1983) *J. Cell Biol. 97*, 48−51.
22. Phillips, W. D., Noakes, P. G., Roberds, S. L., Campbell, K. P., and Merlie, J. P. (1993) *J. Cell Biol. 123*, 729−740.
23. Bowe, M. A., Deyst, K. A., Leszyk, J. D., and Fallon, J. R. (1994) *Neuron 12*, 1173−1180.
24. Campanelli, J. T., Roberds, S. L., Campbell, K. P., and Scheller, R. H. (1994) *Cell 77*, 663−674.
25. Gautam, M., Noakes, P. G., Moscoso, L., Rupp, F., Scheller, R. H., Merlie, J. P., and Sanes, J. R. (1996) *Cell 85*, 525−536.
26. Meier, T., Perez, G. M., and Wallace, B. G. (1995) *J. Cell Biol. 131*, 441−451.

27. Ross, A. F., Rapuano, M., Schmidt, J. H., and Prives, J. P. (1987) *J. Biol. Chem. 262*, 14640−14646.
28. Laemmli, U. K. (1970) *Nature 227*, 280−285.
29. England, P. J., and Walsh, D. A. (1976) *Anal. Biochem. 25*, 429−435.
30. Smith, M. M., Merlie, J. P., and Lawrence, J. C. (1987) *Proc. Natl. Acad. Sci. U.S.A. 84*, 6601−6605.
31. Nef, P., Mauron, A., Stalder, R., Alliod, C., and Ballivet, M. (1984) *Proc. Natl. Acad. Sci. U.S.A. 81*, 7975−7979.
32. Frangioni, J. V., and Neel, B. G. (1993) *Anal. Biochem. 210*, 179−187.
33. Boyle, W. J., Van Der Geer, P., and Hunter T. (1991) *Methods Enzymol. 201*, 110−149.
34. Songyang, Z., Blechner, S., Hoagland, N., Hoekstra, M. F., Piwnica-Worms, H., and Cantley, L. C. (1994) *Curr. Biol. 4*, 973−982.
35. Huganir, R. L., and Miles, K. (1989) *Crit. Rev. Biochem. Mol. Biol. 24*, 183−215.
36. Podleski, T. R., and Salpeter, M. M. (1988) *J. Neurobiol. 19*, 167−185.
37. House, C., Wetterhall, R., and Kemp, B. (1987) *J. Biol. Chem. 262*, 772−777.
38. Kwon, Y.-G., Mendelow, M., and Lawrence, D. S. (1994) *J. Biol. Chem. 269*, 4839−4844.
39. Denis, C., Kemp, B., and Zoller, B. (1991) *J. Biol. Chem. 266*, 17932−17936.
40. Hoch, W., Campanelli, J. T., and Scheller, R. H. (1994) *J. Cell Biol. 126*, 1−4.
41. Swope, S. L., Qu, Z., and Huganir, R. L. (1995) *Ann. N.Y. Acad. Sci. 757*, 197−214.
42. Cohen, G. B., Ren, R., and Baltimore, D. (1995) *Cell 80*, 237−248.
43. Margolis, B. (1996) *J. Lab. Clin. Med. 128*, 235−241.
44. Krebs, E. G. (1986) in *The Enzymes* (Boyer, P. D., and Krebs, E. G., Eds.) pp 3−18, Academic Press, New York.
45. Safran, A., Provenzano, C., Sagi-Eisenberg, R., and Fuchs, S. (1990) *Biochemistry 29*, 6730−6734.
46. Miles, K., Anthony, D. T., Rubin, L. L., Greengard, P., and Huganir, R. L. (1987) *Neurobiology 84*, 6591−6595.
47. Miles, K., Greengard, P., and Huganir, R. L. (1989) *Neuron 2*, 1517−1524.
48. Miles, K., and Huganir, R. L. (1988) *Mol. Neurobiol. 2*, 91−124.
49. Huganir, R. L., and Miles, K. (1989) *Crit. Rev. Biochem. Mol. Biol. 24*, 183−215.
50. Sweet, M. T., Carlson, G., Cook, R. G., Nelson, D., and Allis, C. D. (1997) *J. Biol. Chem. 272*, 916−923.
51. Huganir, R. L., Miles, K., and Greengard, P. (1984) *Proc. Natl. Acad. Sci. U.S.A. 81*, 6968−6972.
52. Schroeder, W., Meyer, H. E., Buchner, K., Bayer, H., and Hucho, F. (1991) *Biochemistry 30*, 3583−3588.

BI9802824